

Towards An Accurate Calculation of the Neutralino Relic Density

二瓶 武史 (日大理工)

I. Supersymmetry

1. Introduction

2. Models

① minimal supergravity model

② minimal supersymmetric standard model

II. Dark matter

1. Introduction

2. Calculation of the relic density

3. Results ("Exact" vs "Expansion")

4. Conclusion

I. Supersymmetry

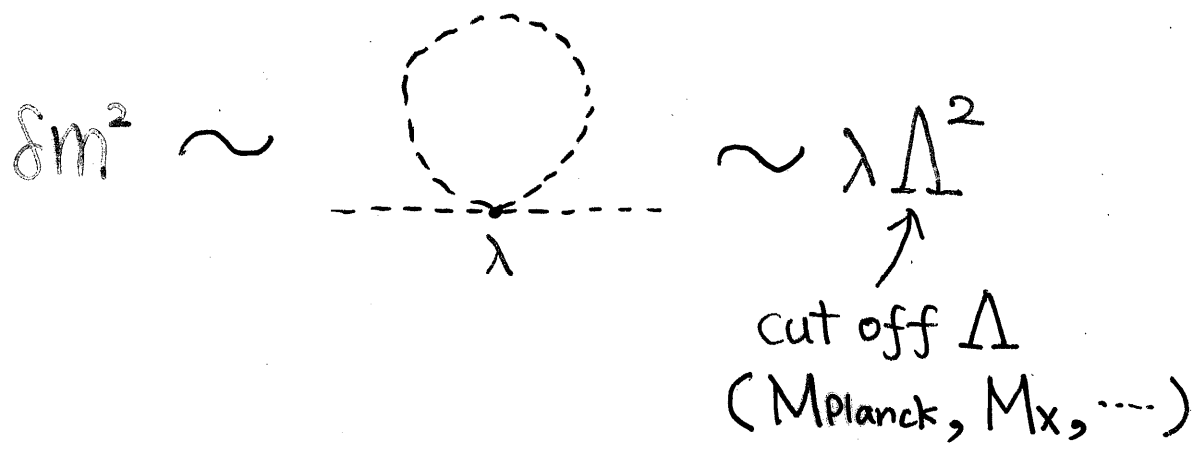
(超对称性)

§1. Introduction

- Standard Model (SM) $SU(3)_c \times SU(2)_L \times U(1)_Y$
 - Weinberg ('67) & Salam ('68, '72)
 - Gross & Wilczek ('73)

$$\xrightarrow[\langle H \rangle \sim O(100 \text{ GeV})]{\text{SSB}} SU(3)_c \times U(1)_{em}$$

- "Problem" of elementary scalar
 scalar mass² ← quadratic divergence



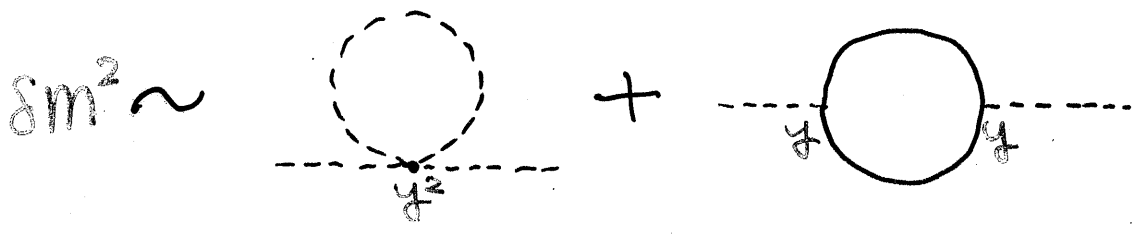
$$M_{\text{phys}}^2 = m_0^2 + \delta m^2$$

$O(100 \text{ GeV}^2) \rightarrow$ unnatural fine tuning?

It is difficult to explain $M_{\text{phys}} \sim O(100 \text{ GeV})$
 unless $\Lambda \sim O(10^{2-3} \text{ GeV})$

→ The theory beyond SM
 should have no quadratic div.

• Supersymmetry (SUSY) Wess & Zumino ('74)
boson ↔ fermion



$\delta m^2 \sim \underbrace{y^2 \Lambda^2 - y^2 \Lambda^2}_{\text{cancellation}} + (\log \text{ div. })$

○ { Λ^2 cancellation ← superpartner
gauge coupling unification ← MSSM

$\sqrt{\frac{5}{3}} g_1 = g_2 = g_3$ Langacker & Luo ('91)

$M_x \sim 10^{16} \text{ GeV} \rightarrow \text{SUSY GUT}$ { Dimopoulos & Georgi ('81)
Sakai ('81)

SUSY must be broken ← $m_{\tilde{e}} \gg m_e$

Soft SUSY breaking ---- SUSY but does not reintroduce Λ^2 div.
 $m_{\tilde{f}} \neq m_f$

$\delta m^2 \sim \underbrace{y^2 (m_{\tilde{f}}^2 - m_f^2)}_{O(m_w^2)} + (\log \text{ div. })$

$\rightarrow m_{\text{SUSY}} \sim 10^{2-3} \text{ GeV}$

What is the origin of Soft breaking?



- Chamseddine, Arnowitt & Nath ('82)
- Barbieri, Ferrara & Savoy ('82) 4

• Supergravity (SUGRA) = local SUSY

$$\boxed{\text{SUGRA}(N=1) \xrightarrow[M_{\text{Planck}}]{\text{SSB}} \text{SUSY} \oplus \text{soft breaking}}$$

$$\Phi_I = \{z_i, \varphi_a\}$$

hidden fields

observable fields

↘ Dynamical SUSY breaking

Superpotential

$$W(\Phi) = h(z_i) + g(\varphi_a) \leftarrow \text{separated}$$

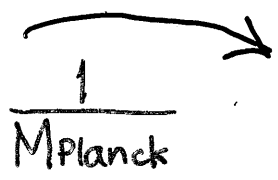
Kähler potential

$$K(\Phi, \Phi^*) = z_i^* z_i + \varphi_a^* \varphi_a \leftarrow \text{minimal}$$

hidden sector

$$\langle F_z \rangle \neq 0$$

SSB



observable sector

$$\mathcal{L}_{\text{SUSY}} + \mathcal{L}_{\text{soft}}$$

$$m_0^2 \phi_a^* \phi_a, A \phi_a \phi_b \phi_c$$

$$B \phi_a \phi_b, \frac{1}{2} M \lambda^\alpha \lambda^\alpha$$

$$m_{\text{SUSY}} \sim \frac{\langle F_z \rangle}{M_{\text{Planck}}}$$

- Gravity included naturally
 - Vanishing cosmological constant
 - No massless Goldstino ($m_{3/2} \neq 0$)
 - Universal scalar mass \leftarrow "if gravity is flavor blind"
 - Radiative breaking of $SU(2)_L \times U(1)_Y$
- ↗ large λ_t ($60 \text{ GeV} \lesssim m_t \lesssim 180 \text{ GeV}$)

- Inoue et al. ('82)
- Ibáñez & Ross ('82)

\longleftrightarrow heavy top $m_t \approx 180 \text{ GeV}$
LEP & CDF

37のゲージ結合定数

の統一は可能！ — くりこみ群方程式

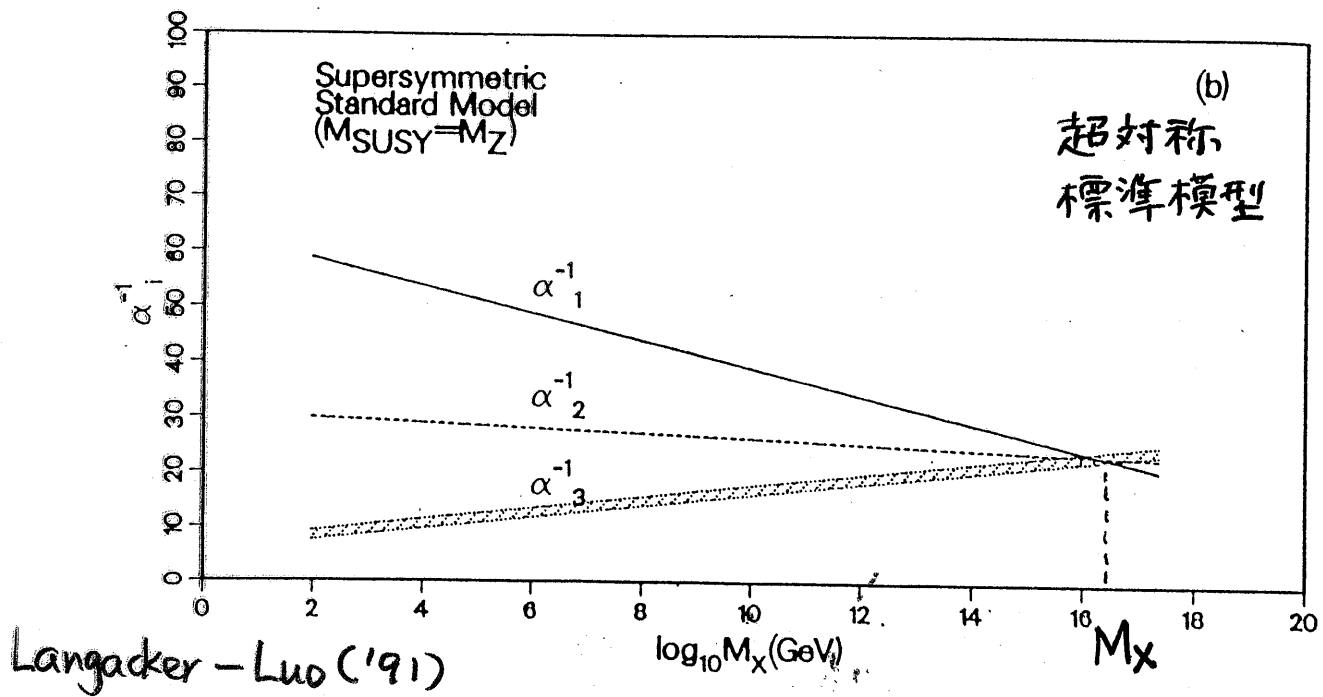
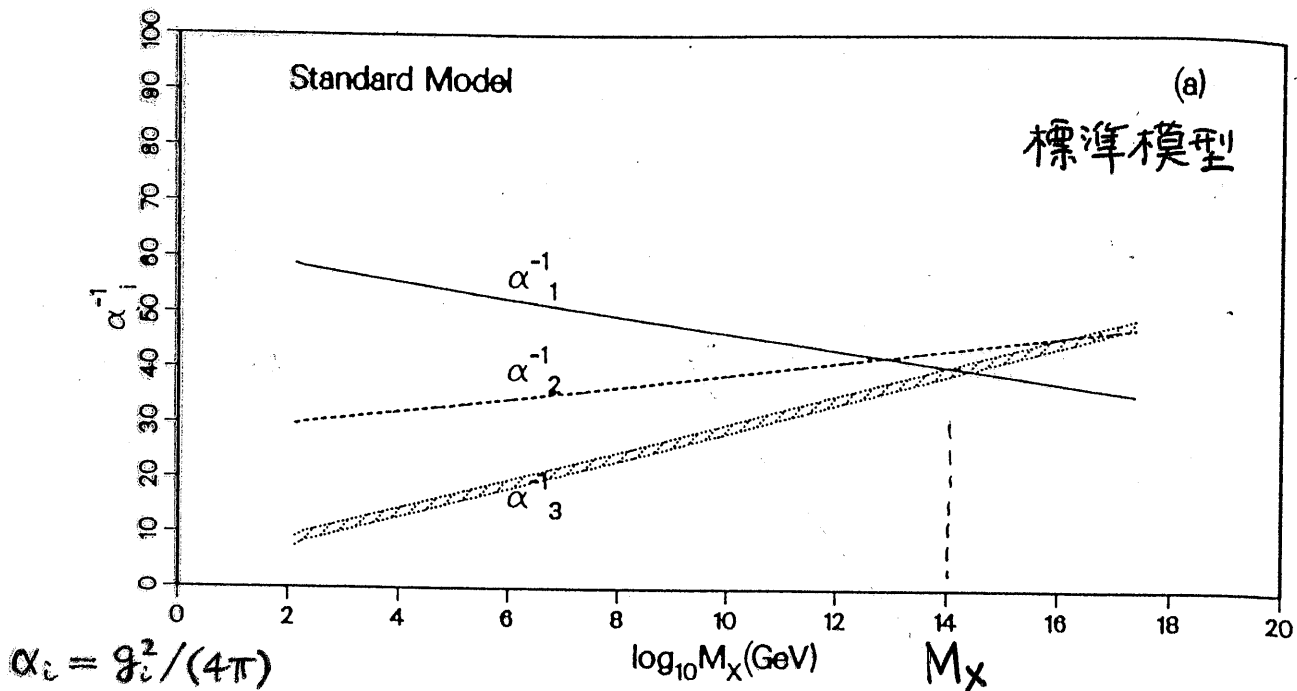


FIG. 3. (a) Running couplings in the standard model. (b) Running couplings in the MSSM with two Higgs doublets for $M_{SUSY} = M_Z$. The corresponding figure for $M_{SUSY} = 1$ TeV is almost identical.

大統一スケール $M_x \approx 2 \times 10^{16}$ GeV において

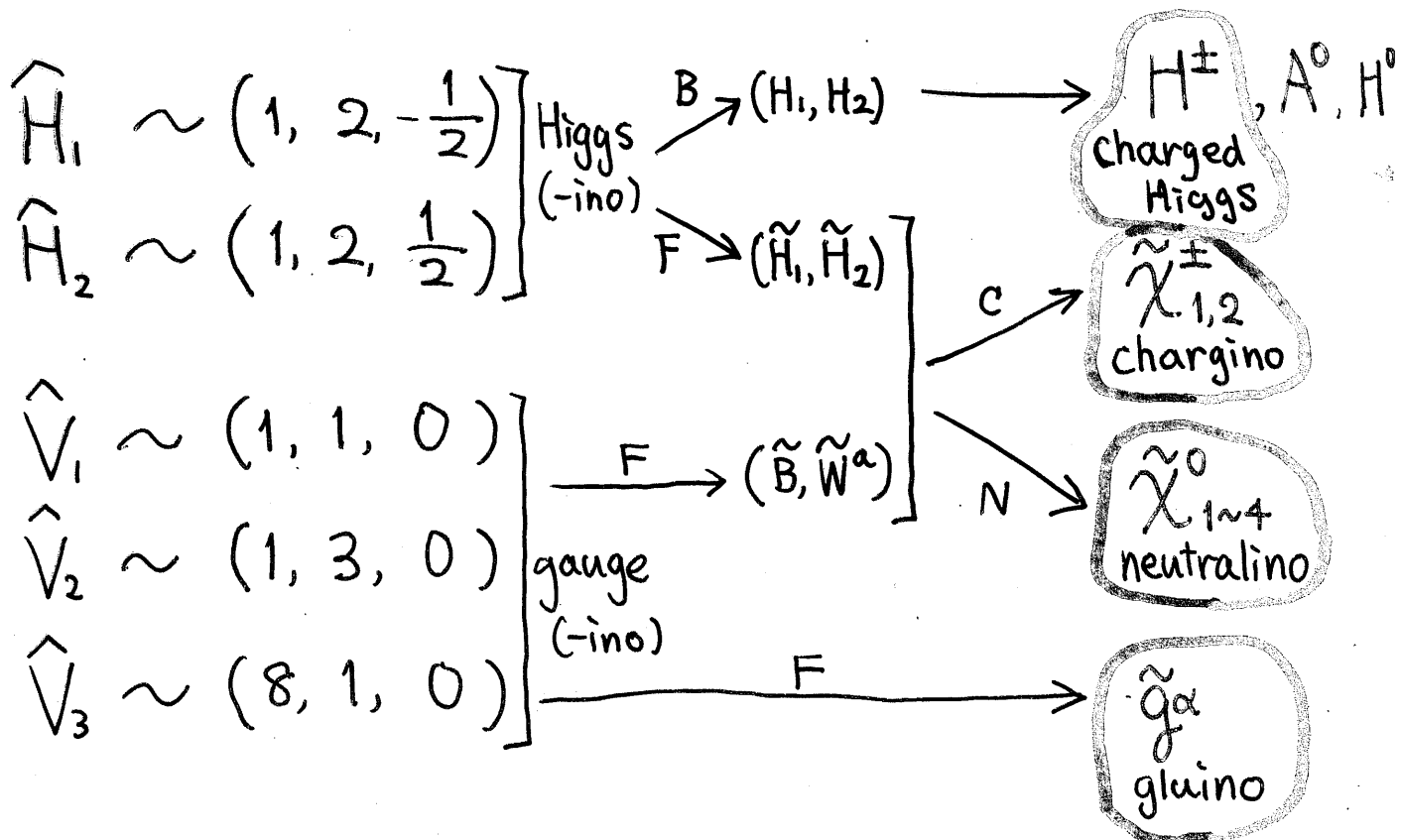
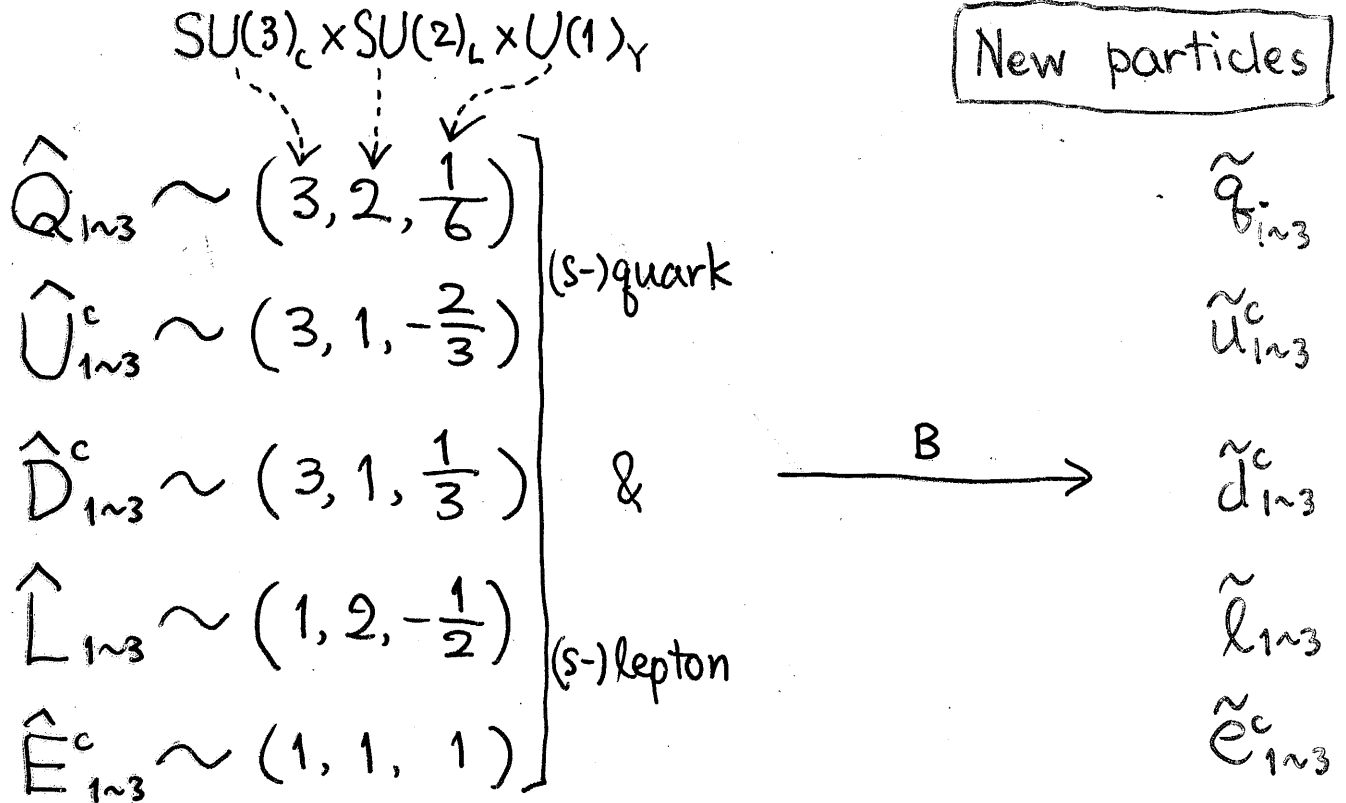
ゲージ相互作用の統一が起こりうる。

→ X, Hc, Σ の質量 ~ O(M_x)

§2. The minimal SUGRA model

- Effective theory below M_{Planck}

Particle content ← minimal SUSY SM



Lagrangian

1) $\mathcal{L}_{\text{SUSY}}$

superpotential

$$\hat{W} = (\lambda_U)_{ij} \hat{H}_2 \hat{U}_i^c \hat{Q}_j + \overset{\text{Yukawa } (i,j=1,2,3)}{\downarrow} (\lambda_D)_{ij} \hat{H}_1 \hat{D}_i^c \hat{Q}_j \\ + (\lambda_L)_{ij} \hat{H}_1 \hat{E}_i^c \hat{L}_j + \mu \hat{H}_1 \hat{H}_2 \\ \text{"}\mu\text{-term"}$$

- gauge invariance
- renormalizability
- R-parity

$$\left\{ \begin{array}{l} \text{Particle in SM: } R = +1 \\ \text{superpartner: } R = -1 \end{array} \right.$$

Parameters in $\mathcal{L}_{\text{SUSY}}$

$$g_1, g_2, g_3$$

$$(\lambda_U)_{ij}, (\lambda_D)_{ij}, (\lambda_L)_{ij} \leftarrow \text{determined by} \\ \tan \beta = \frac{\langle H_2^0 \rangle}{\langle H_1^0 \rangle} \\ \text{and } V_{\text{CKM}} \\ \mu$$

2) $-\mathcal{L}_{soft}$

$$\left[= \sum_{\phi: \text{scalar}} m_0^2 \phi^\dagger \phi + \{ A \hat{W}_3(\Phi) + B \hat{W}_2(\Phi) + h.c. \} + \left\{ \sum_a \frac{1}{2} \tilde{M}_a \tilde{\chi}^a \tilde{\chi}^a + h.c. \right\} \right] \leftarrow \text{hidden sector}$$

$$\left. \begin{aligned} &= (M_Q^2)_{ij} \tilde{q}_{iL}^\dagger \tilde{q}_{jL} + (M_U^2)_{ij} \tilde{u}_{iR}^\dagger \tilde{u}_{jR} \\ &+ (M_D^2)_{ij} \tilde{d}_{iR}^\dagger \tilde{d}_{jR} + (M_L^2)_{ij} \tilde{l}_{iL}^\dagger \tilde{l}_{jL} \\ &+ (M_E^2)_{ij} \tilde{e}_{iR}^\dagger \tilde{e}_{jR} + M_{H_1}^2 |H_1|^2 + M_{H_2}^2 |H_2|^2 \end{aligned} \right\} \text{scalar mass}$$

$$\left. \begin{aligned} &+ \left\{ (A_U)_{ij} H_2 \tilde{u}_{iR}^\dagger \tilde{q}_{jL} + (A_D)_{ij} H_1 \tilde{d}_{iR}^\dagger \tilde{q}_{jL} \right. \\ &\quad \left. + (A_L)_{ij} H_1 \tilde{e}_{iR}^\dagger \tilde{l}_{jL} + h.c. \right\} \end{aligned} \right\} \text{"A-term"}$$

$$+ \left\{ B \mu H_1 H_2 + h.c. \right\} \leftarrow \text{"B-term"}$$

$$+ \left\{ \frac{1}{2} M_1 \tilde{B} \tilde{B} + \frac{1}{2} M_2 \tilde{W}^a \tilde{W}^a + \frac{1}{2} M_3 \tilde{g}^\alpha \tilde{g}^\alpha + h.c. \right\} \leftarrow \text{gaugino mass}$$

Parameters in \mathcal{L}_{soft}

At the GUT scale M_x , $\leftarrow M_{Planck}$

$$(M_Q^2)_{ij} = (M_U^2)_{ij} = \dots = m_0^2 \delta_{ij}$$

$$(A_U)_{ij} = A m_0 (\lambda_U)_{ij}$$

$$(A_D)_{ij} = A m_0 (\lambda_D)_{ij}$$

$$(A_L)_{ij} = A m_0 (\lambda_L)_{ij}$$

$$M_1 = M_2 = M_3 = M_g$$

FCNC OK

m_0

A

M_g

② The minimal supersymmetric standard model (MSSM)

parameters at m_Z

$\tan\beta$
 μ ← Without Radiative ~~EW~~ Condition

m_Q, m_U, m_D, m_L, m_E

M_1, M_2, M_3 ← $M_1 = \frac{5}{3} \tan^2\theta_w \cdot M_2$

A_t, A_b, A_τ ("GUT relation")

m_A



mSUGRA
 $\tan\beta$
 $\text{sgn}(\mu)$
 m_0
 M_g
 A } at $M_x \rightarrow \text{RGE}$

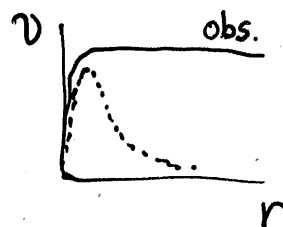
II. Dark Matter

(暗黒物質)

1. Introduction

[1] Dark Matter (DM)

- Rotation curve of spiral galaxies
→ dark matter



- Current observation for $\Omega_i \equiv \rho_i / \rho_c$

— New CMB experiments
(Boomerang, MAXIMA)

$$\Omega_{\text{tot}} = \Omega_M + \Omega_\Lambda \approx 1$$

$$\Omega_M = \Omega_{\text{baryon}} + \Omega_{\text{CDM}}$$

$$= 0.3 \pm 0.1$$

← Dodelson - Knox (1999)

$$\downarrow \Omega_{\text{baryon}} = 0.05 \text{ (BBN)}$$

$$\Omega_{\text{CDM}} = 0.25 \pm 0.1$$

- Hubble constant $H = \dot{a}/a$

$$H_0 \equiv 100 h \text{ km/s/Mpc}$$

$$= (74 \pm 4 \pm 7) \text{ km/s/Mpc}$$

← W. Freedman (2000)

$$\rightarrow h \approx 0.7$$

$$\Omega_{\text{CDM}} h^2 = 0.13 \pm 0.05$$

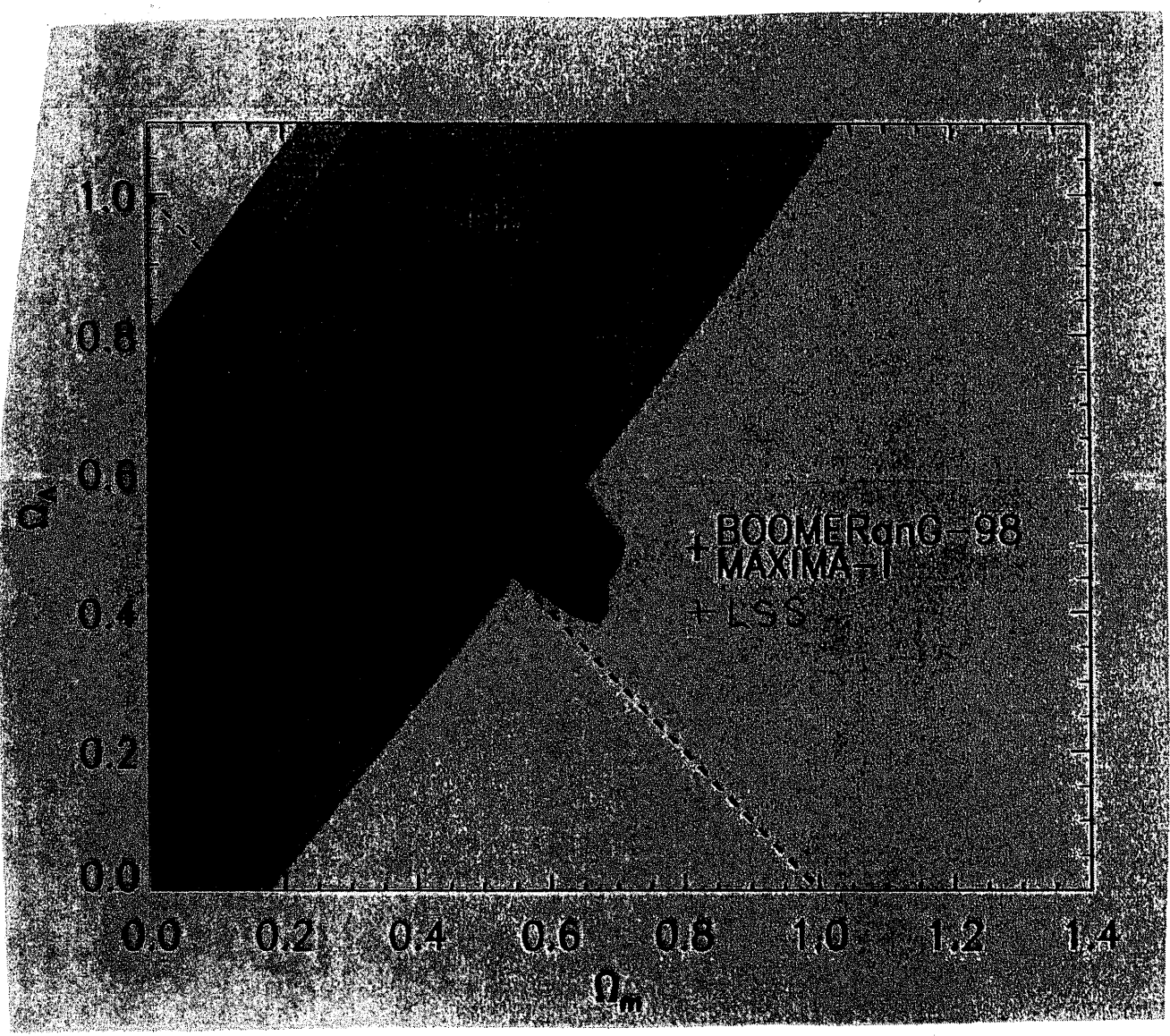
In the following, we use

$$0.1 < \Omega h^2 < 0.3$$

→ Precise calculation of $\Omega_{\text{CDM}}^{\text{theor}}$
becomes important

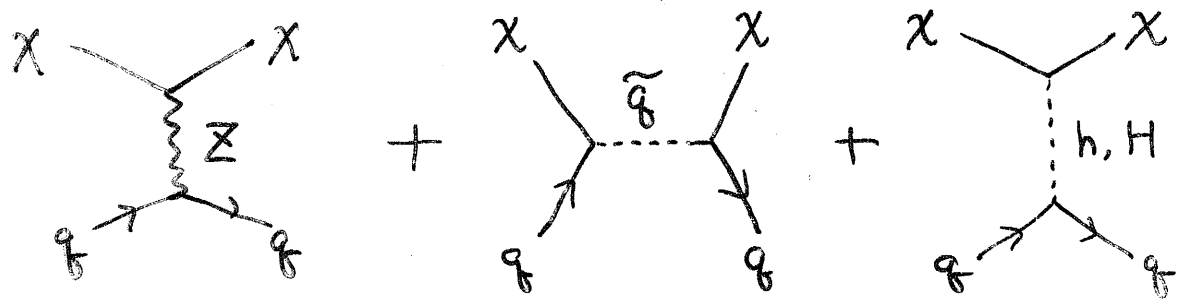
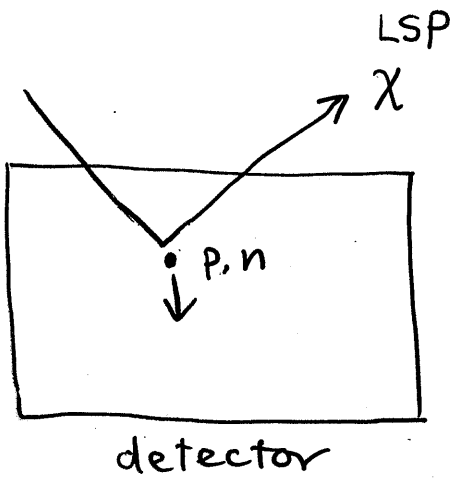
("MAP"
"Planck")

Jaffe et al.
(ICHEP 2000)



• Direct detection of dark matter

Goodman-Witten ('85)



→ $\sigma_{\chi N}$

→ detection rate R

Mandic - Pierce
 - Gondolo - Murayama
 (hep-ph/0008022)

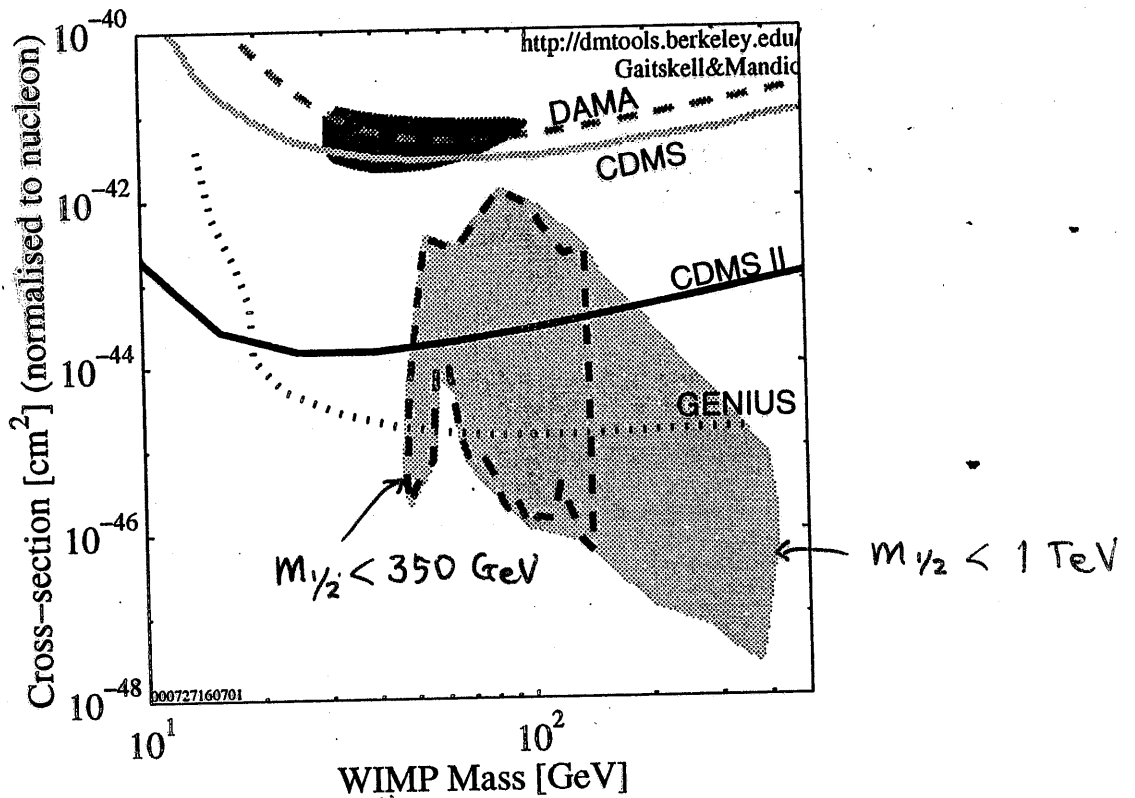


FIG. 2. The cross section for spin-independent χ -proton scattering is shown. A relatively conservative relic density cut is applied, $0.025 < \Omega h^2 < 1$. Current accelerator bounds, including $b \rightarrow s + \gamma$ are imposed through the DarkSUSY code. The darker region is the DAMA allowed region at 3σ CL. The dashed curve is the DAMA 90% CL exclusion limit from 1996 (obtained using pulse-shape analysis). The lighter solid curve is the current CDMS 90% CL exclusion limit, the darker solid curve is the projected exclusion limit for CDMS II experiment and the dotted curve is the projected exclusion limit for the GENIUS experiment. The lighter shaded region is the result of this paper. It represents models allowed within the mSUGRA framework for the constraint $m_{1/2} < 1$ TeV. The closed dashed curve inside this region bounds the region of models allowed in the mSUGRA framework for the constraint $m_{1/2} < 350$ GeV.

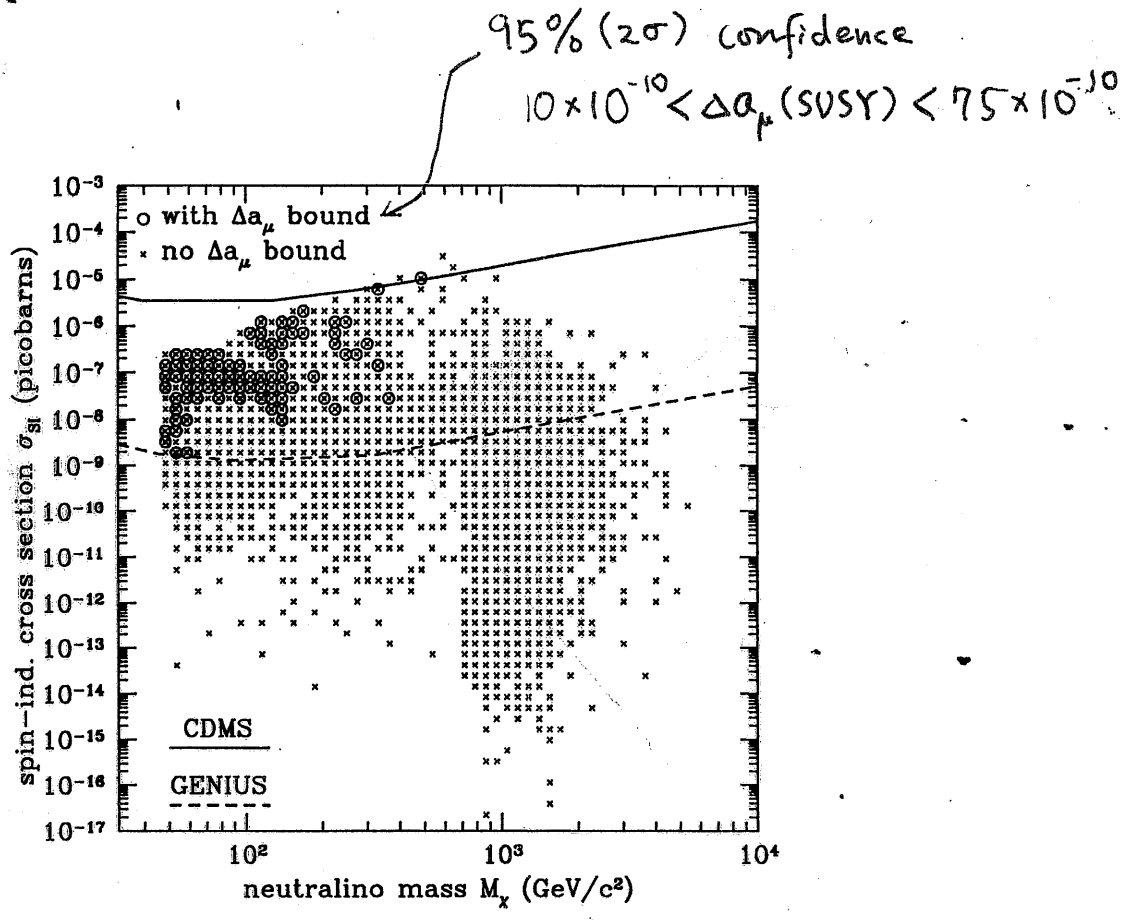
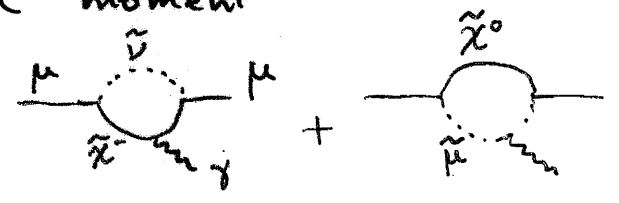


FIG. 2. Astrophysical detectability of SUSY models. In all plots, small crosses indicate cosmologically interesting models, and crossed circles indicate such models that pass the $\Delta a_\mu(\text{SUSY})$ cut. In the top left we plot the spin-independent cross section for neutralino-proton scattering, combined with the CDMS bound and the reach of GENIUS. In the top right we plot the rate of through-going muons in a neutrino telescope for the annihilations in the Sun, with the BAKSAN and SuperKamiokande bounds, and the reach of a km^2 telescope. In the bottom left, we plot a similar rate for neutrinos from the center of the Earth. In the bottom right we plot the intensity of the gamma ray lines in the direction of the galactic center, with the future reach of the VERITAS experiment [28].

muon anomalous magnetic moment

$$a_\mu = \frac{(g-2)_\mu}{2}$$



$$a_\mu^{\text{exp}} - a_\mu^{\text{SM}} = (43 \pm 16) \times 10^{-10} \quad \dots \quad 2.6 \sigma \text{ aZL}$$

↑
 Brookhaven E821
 の結果を入れた世界平均

[2] Supersymmetry (SUSY)

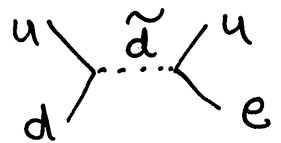
→ candidates for DM

SUSY — gauge hierarchy problem
gauge coupling unification (MSSM)

X #B conservation is not automatic

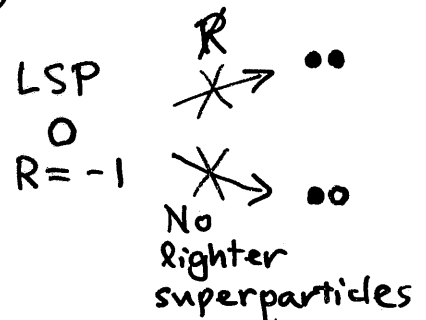
→ R-parity to avoid rapid proton decay

(R = +1 for ordinary particles
R = -1 for super partners)



→ Lightest Super Particle (LSP)

is stable



In the minimal SUGRA model,

mostly, LSP is the lightest neutralino

$$LSP = \chi_1^0$$

$$= \underbrace{N_{11} \tilde{B} + N_{12} \tilde{W}_3}_{\text{gauginos}} + \underbrace{N_{13} \tilde{H}_1^0 + N_{14} \tilde{H}_2^0}_{\text{Higgsinos}}$$

→ candidate for dark matter

MSSM

- gauge group $SM = SU(3) \times SU(2) \times U(1)$
- particle contents

spin = 0	1/2	1
$\tilde{q}, \tilde{u}, \tilde{d}$ \tilde{l}, \tilde{e} <div style="border: 1px dashed black; padding: 5px; display: inline-block;"> H_1, H_2 </div>	q, u, d l, e <div style="border: 1px dashed black; border-radius: 50%; padding: 10px; display: inline-block;"> \tilde{H}_1, \tilde{H}_2 </div> $\tilde{B}, \tilde{W}_a, \tilde{g}_\alpha$	$B_\mu, W_\mu^a, g_\mu^\alpha$

physical Higgses
 h^0, H^0, A^0, H^\pm

mass eigenstates

$$\begin{cases}
 \tilde{H}_1^-, \tilde{H}_2^+, \tilde{W}^1, \tilde{W}^2 \rightarrow \text{chargino } \chi_{1,2}^\pm \\
 \tilde{H}_1^0, \tilde{H}_2^0, \tilde{B}, \tilde{W}^3 \rightarrow \text{neutralino } \chi_{1,2,3,4}^0 \leftarrow
 \end{cases}$$

- superpotential

$$W = (Y_U)_{ij} U_i^c Q_j H_2 + (Y_D)_{ij} D_i^c Q_j H_1 + (Y_E)_{ij} E_i^c L_j H_1 + \mu H_1 H_2$$

R-parity \rightarrow LSP stable (\rightarrow DM)

- soft SUSY breaking

$$\begin{aligned}
 -\mathcal{L}_{\text{soft}} = & \sum_{i,j} (m_\phi^2)_{ij} \phi_i^\dagger \phi_j + \left[\frac{1}{2} \sum_{A=1,2,3} M_A \lambda_A \lambda_A \right. \\
 & + (A_U)_{ij} \tilde{u}_i^c q_j H_2 + (A_D)_{ij} d_i^c q_j H_1 \\
 & \left. + (A_E)_{ij} e_i^c l_j H_1 + B_\mu H_1 H_2 + \text{h.c.} \right]
 \end{aligned}$$

Minimal Supergravity (SUGRA) model

- Boundary conditions at GUT scale

$$\left. \begin{aligned}
 (M_Q^2)_{ij} &= (M_L^2)_{ij} = \dots = m_0^2 \delta_{ij} \\
 M_{H_1}^2 &= M_{H_2}^2 = m_0^2 \\
 (A_{U,D,E})_{ij} &= A (Y_{U,D,E})_{ij} \\
 M_1 &= M_2 = M_3 = m_{1/2}
 \end{aligned} \right\} \begin{array}{l} \text{cf. FCNC} \\ \text{at } M_x \end{array}$$

- RGE

$$M_x \rightarrow m_w$$

- Radiative EW symmetry breaking

$$M_{\text{Higgs}}^2 = m_0^2 > 0 \text{ at } M_x$$

$$\xrightarrow{\text{RGE}} M_{\text{Higgs}}^2 < 0 \text{ at } m_w$$



4 + 1 parameters

$$m_0, m_{1/2}, A, \tan\beta; \text{sgn}(\mu)$$

$$\tan\beta = \langle H_2^0 \rangle / \langle H_1^0 \rangle$$

● Outline of calculation (LSM: $\chi = \chi_1^0$)

$$\Omega_\chi = \rho_\chi / \rho_c, \quad \rho_\chi = m_\chi n_\chi$$

Boltzmann eq

$$\dot{n}_\chi + 3H n_\chi = -\langle \sigma v \rangle (n_\chi^2 - n_\chi^{eq2})$$

where $\sigma = \sigma(\chi\chi \rightarrow \text{ordinary particles})$

$v =$ relative velocity of two χ s

$n_\chi^{eq} = n_\chi$ in thermal equilibrium

$\rightarrow n_\chi$ at present $\rightarrow \Omega_\chi$

● Precise calculation

① all contributions to σ

② exact formula for $\langle \sigma v \rangle$

Gondolo-Germini (1991)

\leftrightarrow expansion $\langle \sigma v \rangle = a + b\chi$, $\chi = T/m_\chi$

③ precise treatment of Boltzmann eq

Srednicki
-Watkins-Olive (1988)

\leftrightarrow approximate solution

④ coannihilation ($\chi\chi' \rightarrow \dots$, $\chi'\chi'' \rightarrow \dots$)

Griest-Seckel (1991)

If $m_{\chi'} \lesssim 1.1 m_\chi$

$$\langle \sigma v \rangle \rightarrow \langle \sigma_{\text{eff}} v \rangle = \sum_{i,j} \frac{n_i^{eq} n_j^{eq}}{n_\chi^{eq2}} \langle \sigma_{ij} v \rangle, \quad m_\chi \rightarrow \sum_i m_i$$

$$\sigma_{ij} = \sigma_{\chi\chi}, \sigma_{\chi\chi'}, \dots$$

$$\chi' = \tilde{t}, \chi_2^0, \chi^\pm, \dots$$

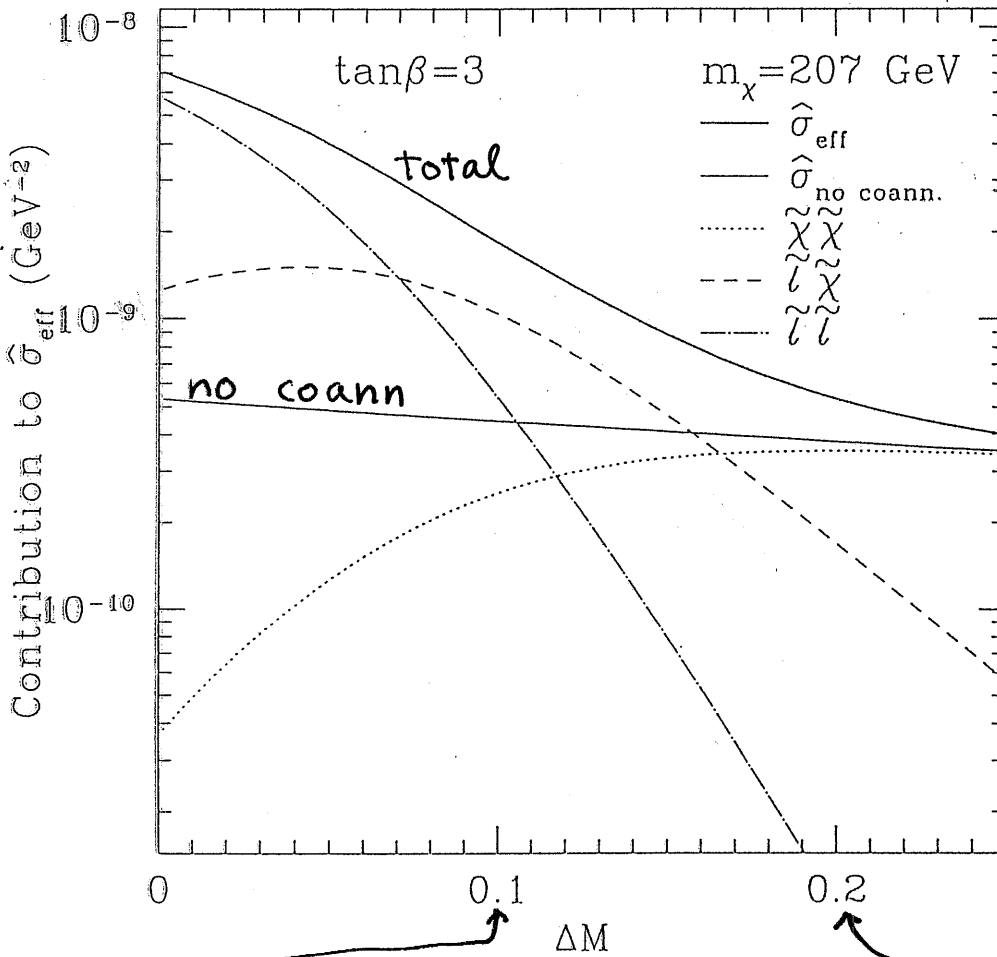
\rightarrow ① + ② in our work

(③, ④ not included yet)

$\chi - \tilde{\tau}$ coannihilation

Ellis-Falk-Olive-Srednicki

hep-ph/9905481



$m_{\tilde{\tau}_R} = 1.1 m_\chi$ $\Delta M \equiv \frac{m_{\tilde{\tau}_R} - m_\chi}{m_\chi}$ $m_{\tilde{\tau}_R} = 1.2 m_\chi$

Figure 5: The separate contributions to the cross sections $\hat{\sigma}_{\text{eff}}$ for $x = T/m_{\tilde{\chi}} \approx 1/23$, as functions of $\Delta M \equiv (m_{\tilde{\tau}_R} - m_{\tilde{\chi}})/m_{\tilde{\chi}}$, with a) $(m_{1/2}, \tan\beta) = (500 \text{ GeV}, 3)$, b) $(500 \text{ GeV}, 10)$, c) $(300 \text{ GeV}, 3)$, and d) $(1000 \text{ GeV}, 3)$.

2. Calculation of relic density

- Lee-Weinberg ('77)⁸
- Goldberg ('83)
- Ellis et al ('83)
- Griest et al ('90)

2-1. Boltzmann eq

$$\dot{n}_\chi + 3Hn_\chi = -\langle\sigma v_{\text{Mol}}\rangle (n_\chi^2 - n_\chi^{\text{eq}2})$$

• Drees-Nojiri ('93)

• Nath-Arnouitt ('93)

• Baer-Brhlik ('96)

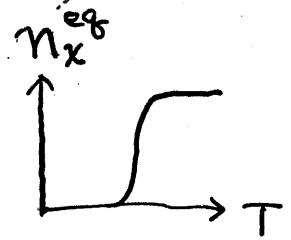
n_χ : neutralino number density
 $H = \dot{a}/a$: Hubble parameter

$$v_{\text{Mol}} = \frac{1}{E_1 E_2} \sqrt{(p_1 \cdot p_2)^2 - m_1^2 m_2^2}$$

$\sigma = \sigma(\chi\chi \rightarrow \text{ordinary particles})$

$$T \gg m_\chi$$

$$\downarrow n_\chi = n_\chi^{\text{eq}}$$



$$T = T_F \quad \dots \quad T_F \text{ is determined by}$$

$$\dot{n}_\chi^{\text{eq}} + 3Hn_\chi^{\text{eq}} = -\langle\sigma v_{\text{Mol}}\rangle n_\chi^{\text{eq}2} \quad \dots \quad \textcircled{1}$$

Typically $T_F \sim m_\chi/20$

$$\downarrow n_\chi + 3Hn_\chi = -\langle\sigma v_{\text{Mol}}\rangle n_\chi^2 \quad \dots \quad \textcircled{2} \quad \leftarrow n_\chi^{\text{eq}} \approx 0$$

$$T = T_0 : n_\chi = n_{\chi 0}$$

$$\textcircled{1} \Rightarrow x_F^{-1} = \ln \left(\frac{m_\chi}{2\pi^3} \sqrt{\frac{45}{29 * G_N}} \langle\sigma v_{\text{Mol}}\rangle_{x_F} x_F^{1/2} \right)$$

$$x_F \equiv T_F / m_\chi$$

$$\textcircled{2} \Rightarrow \rho_{\chi 0} = 1.66 \frac{1}{M_p} \left(\frac{T_\chi}{T_\gamma} \right)^3 T_\gamma^3 \sqrt{g_*} \frac{1}{\int_0^{x_F} dx \langle\sigma v_{\text{Mol}}\rangle}$$

$$\Omega_\chi = \rho_{\chi 0} / \rho_c, \quad \rho_c \approx 10^{-5} h^2 \text{ GeV}/\text{cm}^3$$

Jungman-Kamionkowski-Griest (1996)

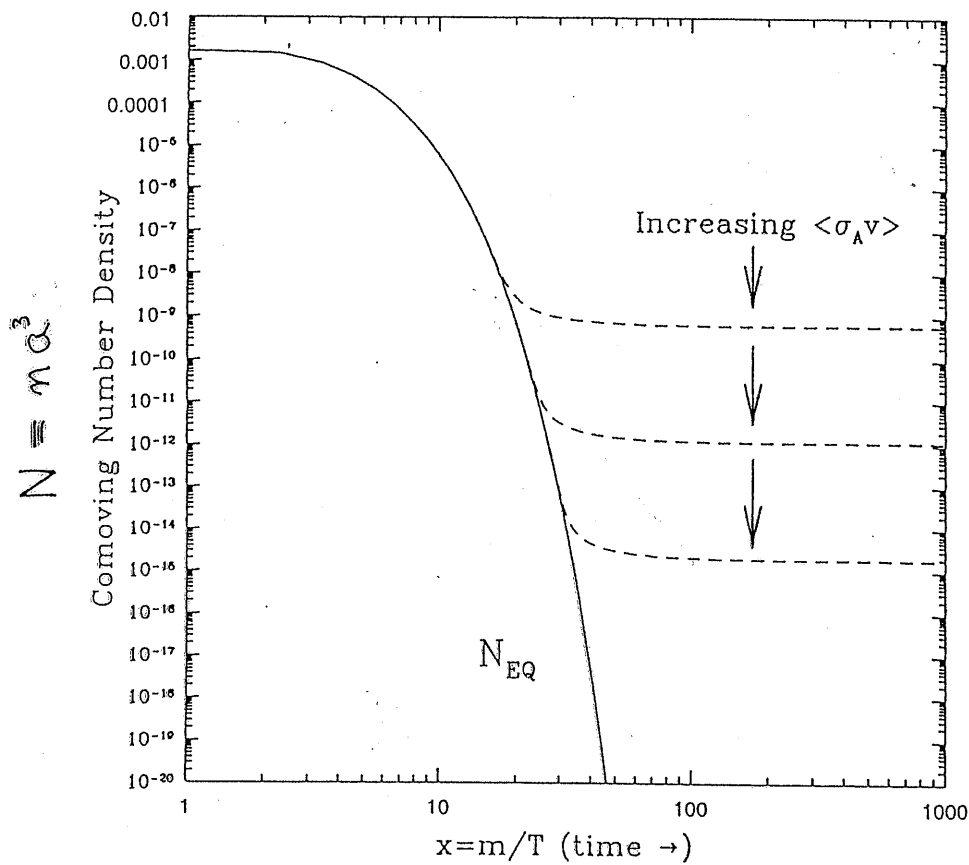


Fig. 4. Comoving number density of a WIMP in the early Universe. The dashed curves are the actual abundance, and the solid curve is the equilibrium abundance. From [31].

Kolb - Turner ('89)

2-2. cross section

• Diagrams

$$\sigma = \sigma(\chi\chi \rightarrow \text{all})$$

where

$$\text{"all"} = f\bar{f},$$

$$W^+W^-, Z\bar{Z},$$

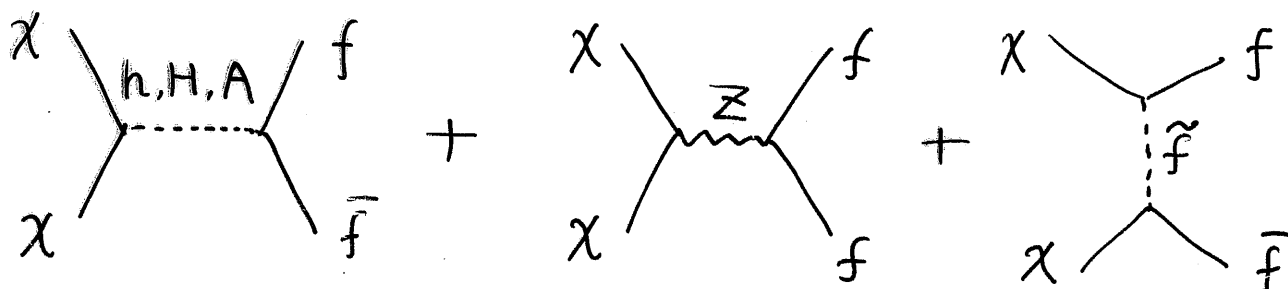
$$hh, hH, HH, hA, HA, AA, H^+H^-,$$

$$Zh, ZH, ZA, W^+H^+$$

• Dominant mode

$$\chi\chi \rightarrow f\bar{f}$$

$$\left(\begin{array}{l} \text{mSUGRA} \\ m_{\tilde{e}} < m_{\tilde{g}} \\ \chi\chi \rightarrow l_R \bar{l}_R \text{ dominant} \end{array} \right)$$



2-2 cross section

● Feynman diagrams contributing to $\sigma(\chi\chi \rightarrow \dots)$

	s-channel	t&u-channel
$\textcircled{\chi\chi} \rightarrow f\bar{f}$	h, H, A, Z 	\tilde{f}_{1-6}
$\chi\chi \rightarrow$ hh hH HH hA HA AA H^+H^-	$\left. \begin{array}{l} \\ \\ \\ \end{array} \right\} h, H$ $\left. \begin{array}{l} \\ \\ \end{array} \right\} A, Z$ h, H h, H, Z	$\left. \begin{array}{l} \\ \\ \\ \end{array} \right\} \chi_{1-4}^0$ $\chi_{1,2}^\pm$
$\chi\chi \rightarrow W^+W^-$ ZZ	h, H, Z h, H	$\chi_{1,2}^\pm$ χ_{1-4}^0
$\chi\chi \rightarrow Zh$ ZH ZA $W^\pm H^\mp$	$\left. \begin{array}{l} \\ \\ \end{array} \right\} Z, A$ h, H h, H, A	$\left. \begin{array}{l} \\ \\ \end{array} \right\} \chi_{1-4}^0$ $\chi_{1,2}^\pm$

\uparrow
 s-channel
 (h, H, A, Z)

Analytic Expressions
 $\left. \begin{array}{l} f\bar{f} \\ hh\dots \\ ww\dots \end{array} \right\}$ in literatures

2-3. Thermal average $\langle \sigma v \rangle$

[1] Exact formula Gondolo - Germini (191)

$$\langle \sigma v_{\text{Mol}} \rangle = \frac{\int d^3 p_1 d^3 p_2 \sigma v_{\text{Mol}} e^{-E_1/T} e^{-E_2/T}}{\int d^3 p_1 d^3 p_2 e^{-E_1/T} e^{-E_2/T}}$$

$$= \frac{1}{8m_x^4 T K_2(m_x/T)} \int_{4m_x^2}^{\infty} ds \sigma(s-4m_x^2) \sqrt{s} K_1(\sqrt{s}/T)$$

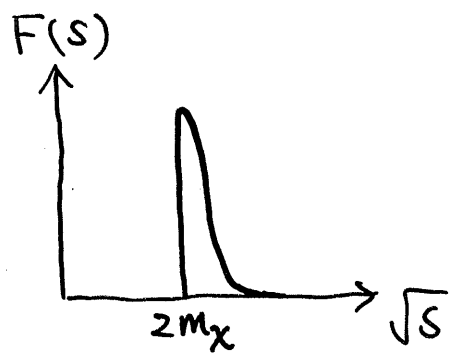
$T_F \ll m_x$: Boltzmann distribution

• Behavior of integrand of $\langle \sigma v \rangle$

$\sqrt{s}/T \gg 1 \quad \leftarrow \quad T \lesssim \frac{m_x}{20}, \quad \sqrt{s} \geq 2m_x$

\downarrow
 $K_1(\sqrt{s}/T) \sim \sqrt{\frac{\pi T}{2\sqrt{s}}} e^{-\frac{\sqrt{s}}{T}}$: dies away quickly with increasing \sqrt{s}

\downarrow
 $\langle \sigma v_{\text{Mol}} \rangle \sim \int_{4m_x^2}^{4m_x^2(1+\delta)} ds \quad \sigma \times F(s)$



[2] Expansion

Srednicki-Watkins-Olive
(1988)

- In lab frame

$$\sigma V_{\text{lab}} = \frac{1}{64\pi^2(s-2m_x^2)} \beta_f \int d\Omega \sqrt{|m^2|}$$

where

$$\beta_f = \sqrt{1 - \frac{(m_3+m_4)^2}{s}} \sqrt{1 - \frac{(m_3-m_4)^2}{s}} \quad \chi\chi \rightarrow f_3 f_4$$

- Expansion

$$\sigma V_{\text{lab}} = a^{(0)} + a^{(1)}\epsilon + O(\epsilon^2)$$

where

$$\epsilon = \frac{(E_{1,\text{lab}} - m) + (E_{2,\text{lab}} - m)}{2m}$$

$$= \frac{s - 4m_x^2}{4m_x^2} \quad : \text{kinetic energy per unit mass}$$

$$\langle \sigma V_{\text{Mol}} \rangle = \langle \sigma V_{\text{lab}} \rangle^{\text{lab}}$$

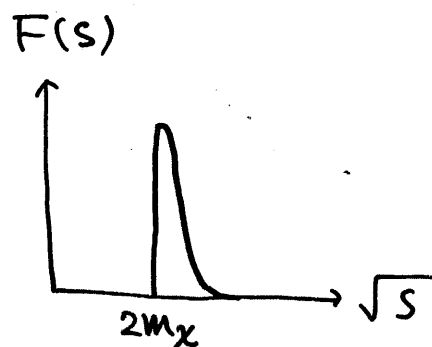
$$= a^{(0)} + \frac{3}{2} a^{(1)} \chi + O(\chi^2) \quad \leftarrow \chi \equiv T/m_x$$

$$= a + b\chi + O(\chi^2)$$

Exact vs Expansion

Naively "expansion" should converge quickly because $F(s)$ decays quickly.

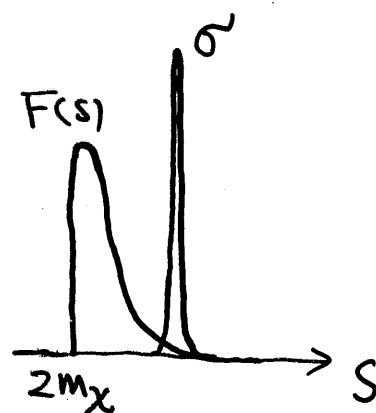
$$\langle \sigma v_{\text{Mol}} \rangle \sim \int_{4m_\chi^2} ds \sigma \times F(s)$$



This is not necessarily true when σ varies rapidly with s

(e.g. near s -pole, threshold of new channel)

- Gondolo - Germini (191)
- Lopez - Nanopoulos - Yuan (193)



Z pole

Lopez-Nanopoulos
-Yuan (1983)

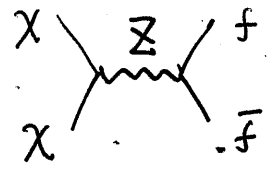
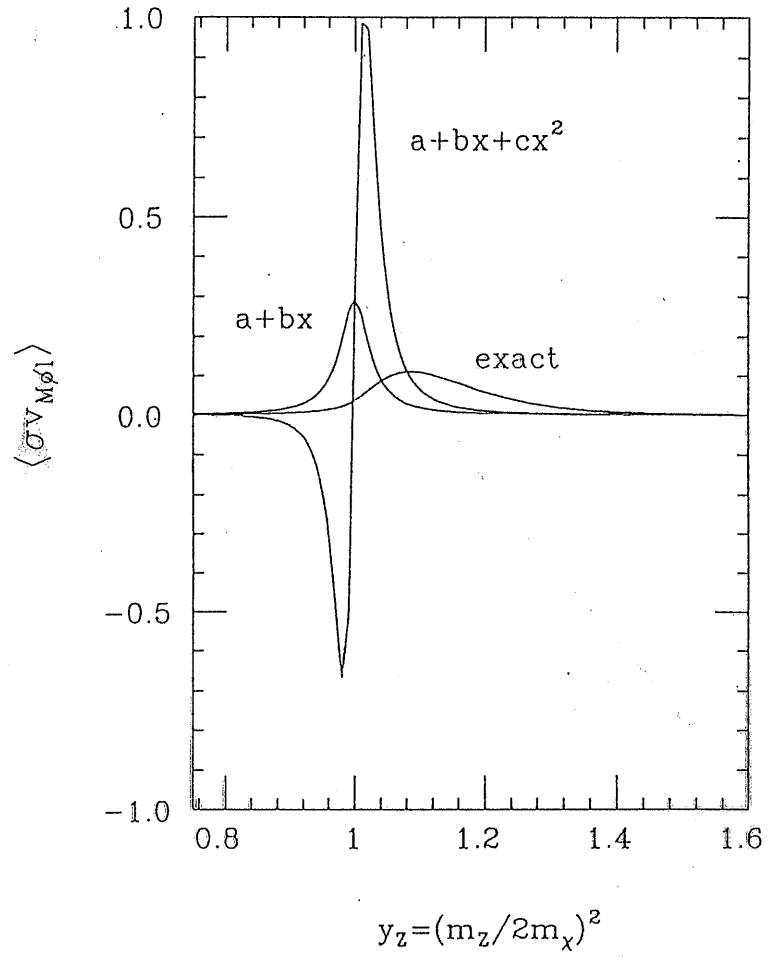


FIG. 1. The thermal average $\langle \sigma v_{M\phi 1} \rangle$ (in arbitrary units) as a function of $y_z = (M_Z/2m_\chi)^2$ for a Z-pole dominance situation. The exact and traditional series-expansion results are shown. Note that the second-order approximation gives negative thermal averaged annihilation cross sections right above the pole.

$$\sigma \sim \frac{1}{(s - m_Z^2)^2} \sim \frac{1}{(4M_\chi^2 - m_Z^2)^2}$$

$s \approx 4M_\chi^2$ $\textcircled{cf} P_Z \approx 2 \text{ GeV}$

σ is enhanced when $2M_\chi \approx m_Z$

3. Results

— "Exact" vs "Expansion"

MSSM

$$\tan\beta = 10$$

$$M_Q = M_U = M_D = M_L = M_E = 500 \text{ GeV}$$

$$M_A = 400 \text{ GeV}$$

$$A_t = A_b = 600 \text{ GeV}$$

$$\mu = -500 \text{ GeV}$$



$$\int_0^{x_F} dx \langle \sigma v_{\text{Mol}} \rangle$$

$$x_F$$

$$\Omega_x h^2$$

$$\Omega_x^{\text{exp}} / \Omega_x^{\text{exact}}$$

} vs M_x

$$J(x_F) = \int_0^{x_F} dx \langle \delta V_{\text{mol}} \rangle$$

Nihei-Roszkowski
-Ruiz
(hep-ph/0102308)

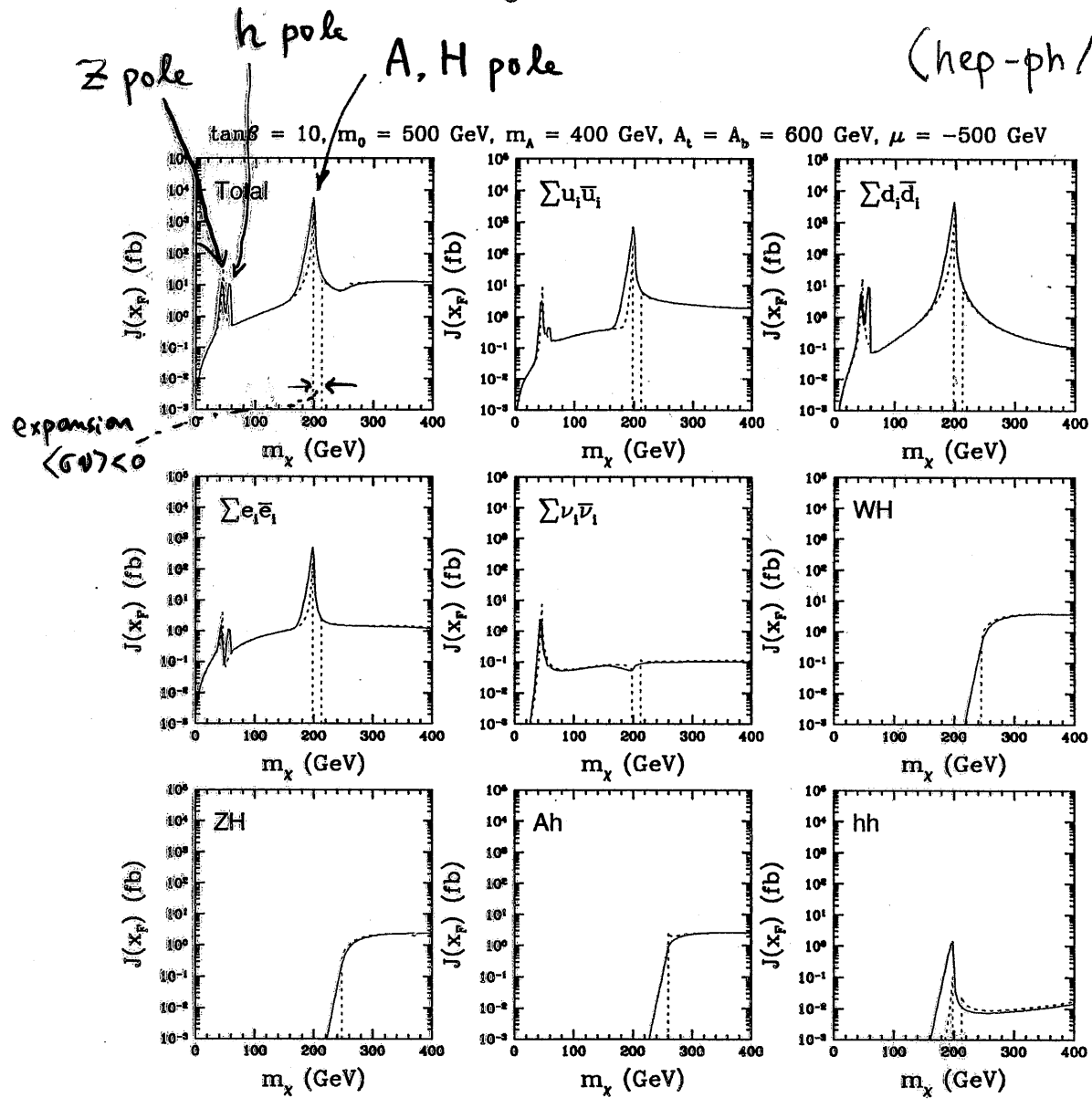


Figure 1: The total value of $J(x_f)$, Eq. (5), and several partial contribution are shown in separate windows as a function of m_χ for $\tan\beta = 10, m_0 \equiv m_Q = m_U = m_D = m_L = m_E = 500 \text{ GeV}, m_A = 400 \text{ GeV}, A_t = A_b = 600 \text{ GeV}$ and $\mu = -500 \text{ GeV}$. The solid lines represent the exact results, while the dotted ones correspond to the expansion (13). Notice that the final states $W^\pm H^\mp, ZH^0$ and Ah , once kinematically allowed, give comparable contributions to the $f\bar{f}$ channels.

WH が dominant になる領域あり！

(\odot $f\bar{f}, WW$)

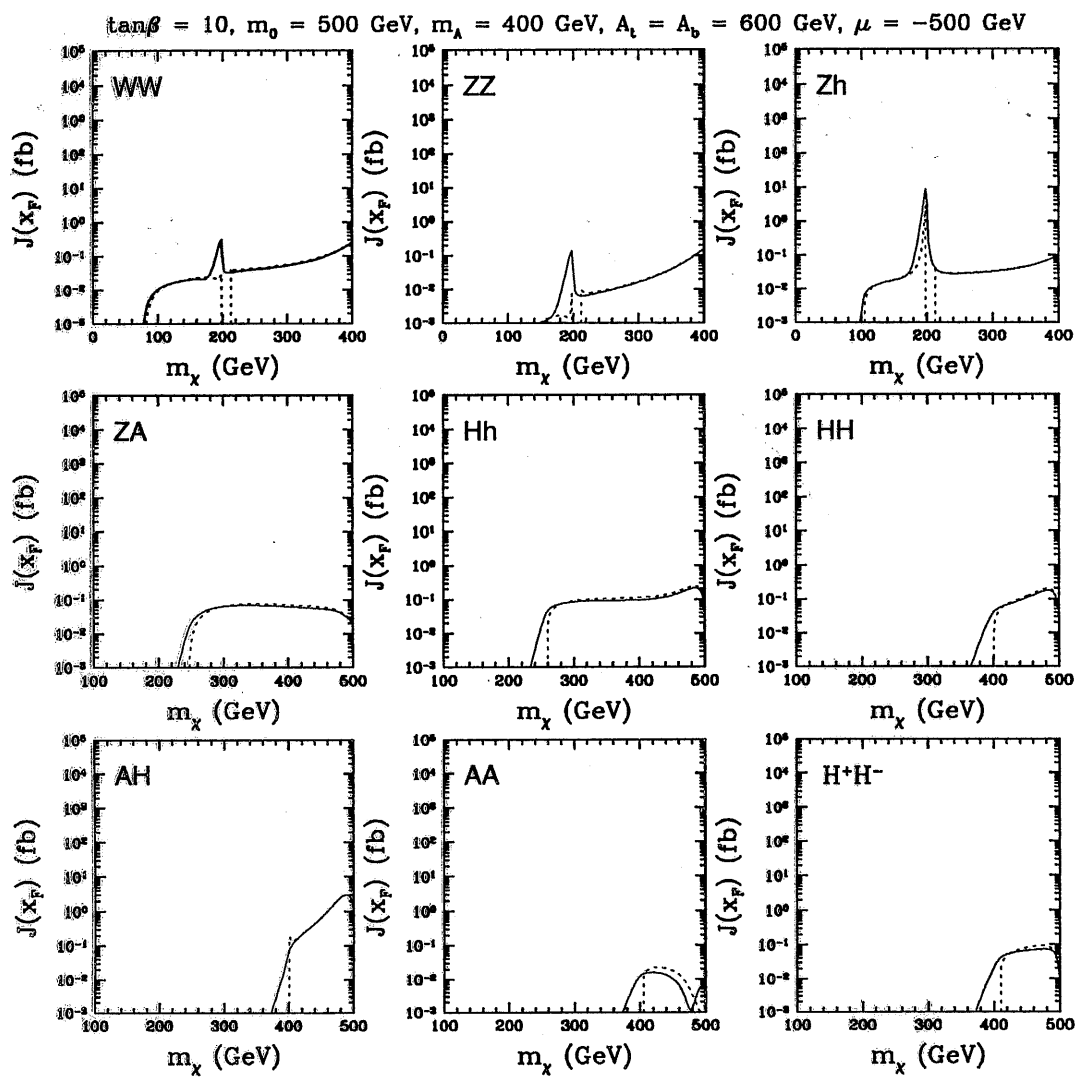


Figure 2: The same as in Fig. 1 but for mostly subdominant channels. Notice that in the lower two rows the horizontal axis has been shifted by 100 GeV.

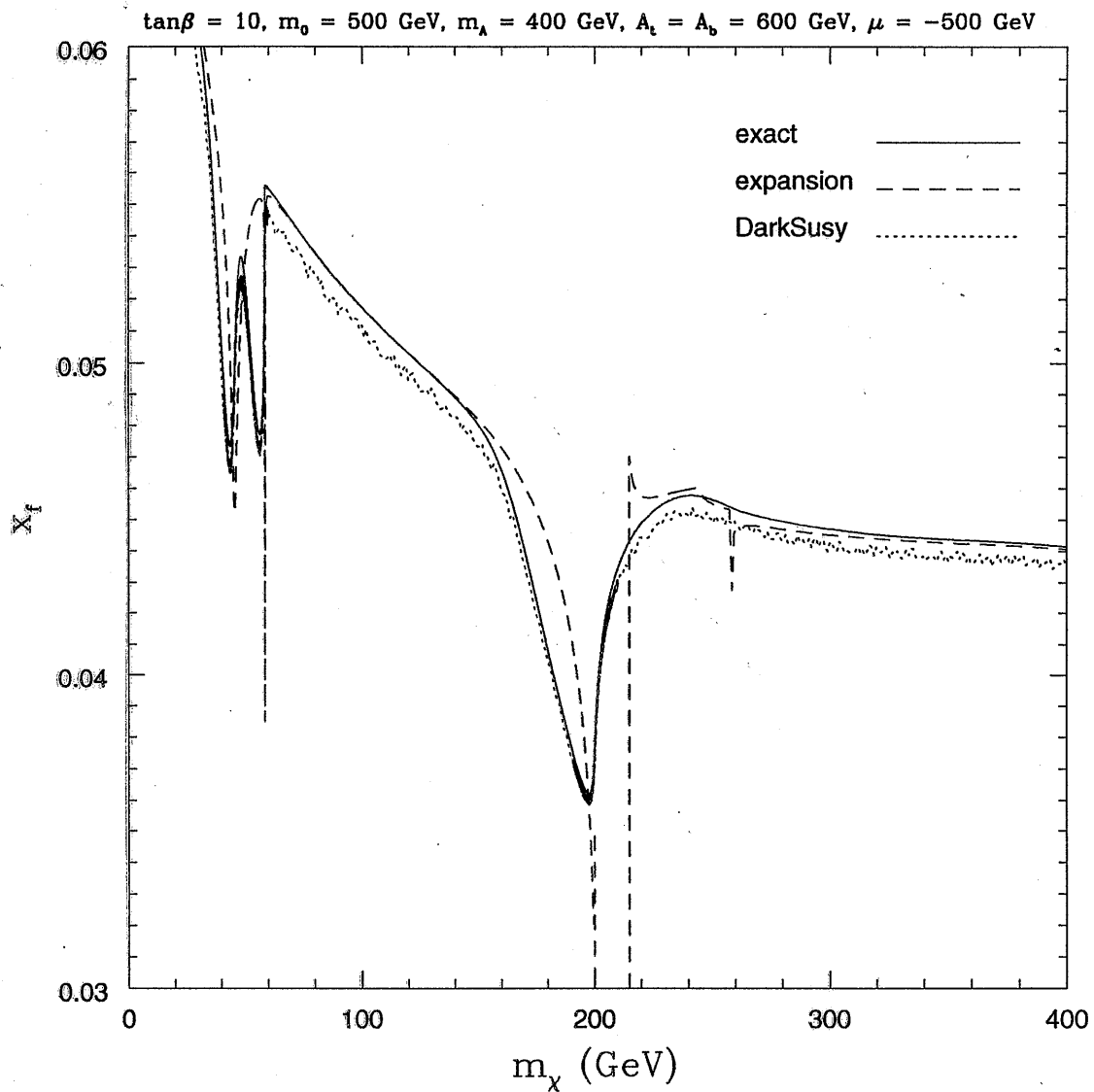


Figure 3: The freeze-out point x_f as a function of m_χ . The solid and dashed lines corresponds to the iterative procedure (3) with $\langle\sigma v_{M\bar{0}1}\rangle$ computed exactly (6) and in terms of the expansion (13), respectively. For comparison, the dotted line has been obtained using DarkSusy.

"Dark SUSY" (numerical code)

Gondolo et al

astro-ph/0012234

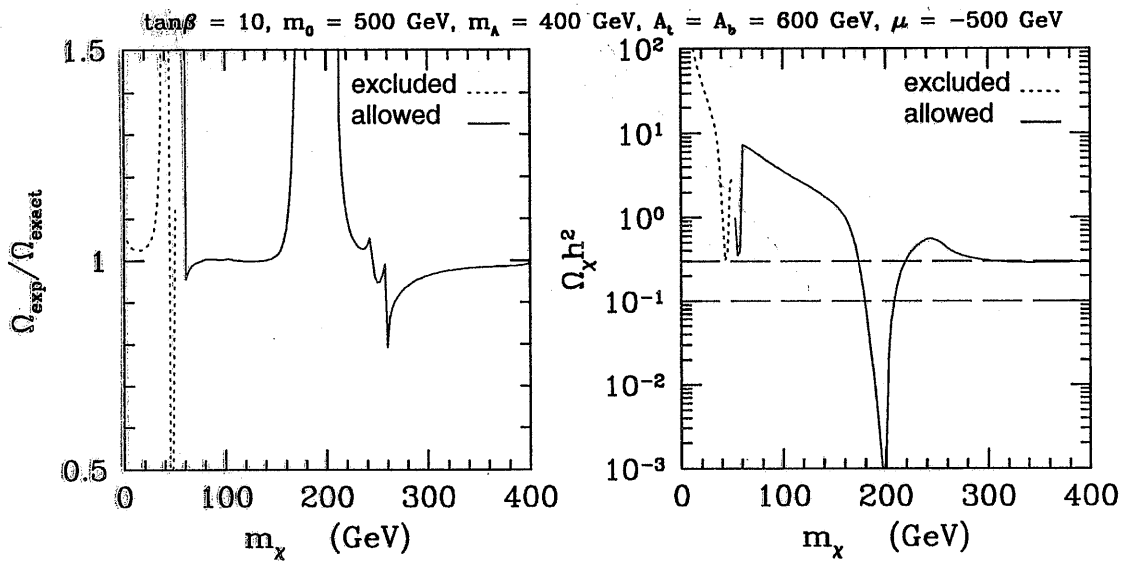


Figure 4: The ratio $\Omega_{\text{exp}}/\Omega_{\text{exact}}$ (a) and the relic density $\Omega_\chi h^2$ (b) for the same choice of parameters as in Fig. 1. The solid (dotted) curves are allowed (excluded) by current experimental constraints. In window (a) the relic abundance in both cases is computed by solving Eq. (3) iteratively and using Eq. (4). In window (b) we show $\Omega_\chi h^2$ is computed using our numerical code. The band between the two horizontal dashed lines corresponds to the cosmologically favoured range $0.1 < \Omega_\chi h^2 < 0.3$.

4. Conclusion

■ Supersymmetry は 標準理論を
越える物理として有望な枠組

■ 実験的検証が不可欠

- LHC等の次世代加速器

- Dark Matter の直接検出
(CDMS II, GENIUS)

- Relic density の制限
↓
(MAP, Planck)

Ω_x の正確な計算が必要

重い Higgs (H, A) の pole の領域では、
比較的広い範囲にわたって $\Omega_{\text{exp}} / \Omega_{\text{exact}}$
が 1 からずれる